HERON
ENGLISH EDITION
No. 2 1963

IR. F. K. LIGTENBERG
with the collaboration of
A. C. VAN RIEL, H. J. VADER and IR. J. VAN LEEUWEN

ANALOGY MODEL FOR STUDYING BUCKLING PHENOMENA IN THE ELASTO-PLASTIC RANGE

U.D.C. 624.075.2

A description is given of an analogy by means of which it is possible, in a relatively simple manner, to gain an insight into the behaviour of axially and eccentrically compressed structural members in the elasto-plastic range. The model was used in the course of an investigation that yielded results which are embodied in Clause 47 of the Netherlands Standards Code of Practice for Reinforced Concrete (G.B.V. 1962) (ultimate-load design). A member loaded in the manner envisaged above is represented by a similarly loaded block (the model) of light material floating in a liquid. By a simple analogy the requisite inferences as to the member under consideration (stresses in sections, etc.) can be drawn from the state of equilibrium into which, in the test, the model is brought by means of appropriate loading.

0 Introduction

The results of an exhaustive investigation of the ultimate-load design of reinforced concrete columns as presently published in this issue (pp. 14 et seq.), are based on an appropriate model analogy. Although this analogy had already been studied by one of the present authors some years ago, an opportunity of applying it for practical purposes had not earlier presented itself.

Now, however, it was found that by this means very satisfactory results could be obtained in a relatively simple manner and with the aid of limited equipment. Also, the analogy presented some worthwhile aspects in support of considerations relating to buckling problems.

Although the analogy is applicable not only to reinforced concrete columns but also to such members made of steel or some other material, its application has hitherto been confined to reinforced concrete columns. Accordingly, the present article more particularly gives a description of the experience that has been gained with these and has yielded the results mentioned in the exordium.

1 Basis of the analogy model

A floating block can be used for representing the behaviour of a section, subjected to bending and direct force, in a manner that can be visualized. Vertical

forces acting upon that block cause it to be submerged so much deeper in the liquid that the force applied to the block is compensated by the upward pressure due to the water displaced.

There is an obvious analogy between the upward hydrostatic pressure and the stress in a section of the same shape, and also between the deflections in relation to the original position of the block and the strains at corresponding points of the section. This will be elucidated with reference to a floating rectangular block (Fig. 1) whose top surface is maintained parallel to the surface of the liquid.

If a downward force N' is exerted upon this block, then the latter will sink so much farther into the liquid (so long as the top surface has not yet reached the surface of the liquid) that the deflection is proportional to the force. When the top surface of the block coincides with the liquid surface the maximum attainable displacement of water – and therefore also the maximum counteracting pressure – is attained. With loads acting in the opposite direction (*i.e.*, upwards) something similar will evidently occur.

The load-deflection diagram is given in Fig. 2. There is obvious agreement with the mechanical properties of a material behaving elastically between two pronounced yield stress levels.

If the model, before testing, is so loaded by an initial force that it is immersed in the liquid to a depth m corresponding to half its thickness, then the horizontal axis in Fig. 2 will be shifted vertically in such a manner as to make the diagram antimetric (see Fig. 3). Furthermore, N' can of course be replaced by the corresponding uniformly distributed compressive stress $\sigma' = \gamma z'$; and N can similarly be replaced by $\sigma = \gamma z$. Dimensionless quantities can be marked off on the axes, as indicated in Fig. 3. If the stress-strain diagram for steel, as assumed in Clause 47, par. 1, of G.B.V. 1962, is likewise plotted as a dimensionless graph (see Fig. 4), Figs. 3 and 4 are seen to be identical. The downward deflection z' and the upward deflection z are analogous to the compressive strain (shortening) ε_a' and to the tensile strain (elongation) ε_a respectively. The half thickness m corresponds to the strain ε_e' associated with the compressive yield point or, alternatively, to the strain ε_e associated with the tensile yield point of the steel.

A stress-strain diagram having the shape of a quadratic parabola can be represented by similar means. For this purpose a model of triangular vertical cross-sectional shape should be employed. In Fig. 5, by way of example, a section of this kind on a rectangular base (triangular prism) is represented. Fig. 6 gives the relation between the load and the downward deflection z' or upward deflection z. If, prior to testing, an initial force is so applied to the prism that the underside thereof just touches the surface of the liquid, then the horizontal axis in Fig. 6 will be shifted vertically by such an amount that Fig. 7 is obtained. The diagram that we get thus is identical with the stress-

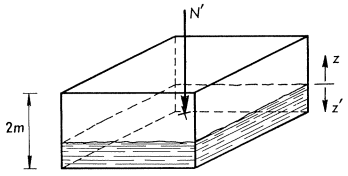

Fig. 1. Axially (*i.e.*, centrally) loaded model.

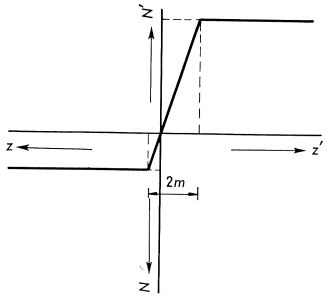

Fig. 2. Relation between N and z for the model in Fig. 1.

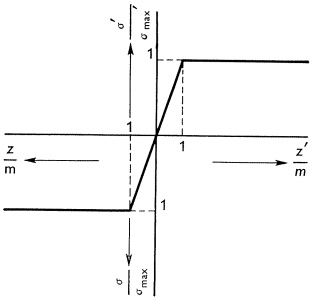

Fig. 3. Same relation as in Fig. 2, but with horizontal axis displaced (dimensionless).

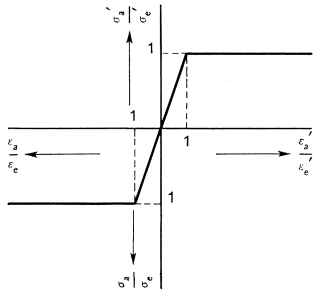

Fig. 4. Stress-strain diagram according to Clause 47, par. 1, G.B.V. 1962 (dimensionless).

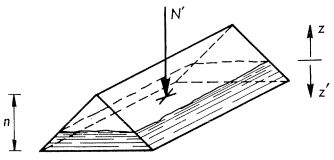

Fig. 5. Axially (*i.e.*, centrally) loaded model.

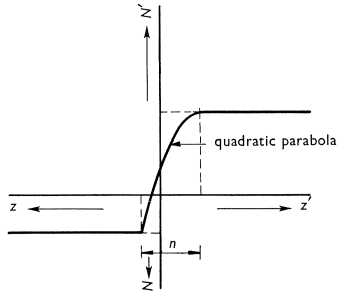

Fig. 6. Relation between N and z for the model in Fig. 5.

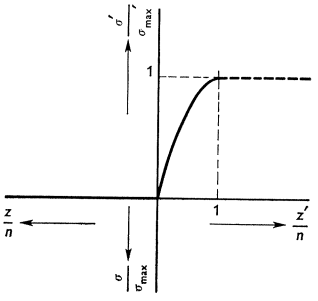

Fig. 7. Same relation as in Fig. 2, but with horizontal axis displaced (dimensionless).

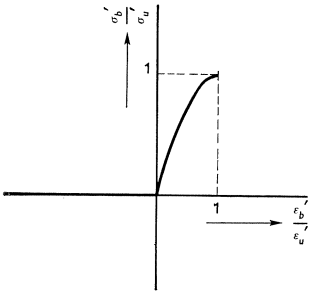

Fig. 8. Stress-strain diagram according to Clause 47, par. 1, G.B.V. 1962 (dimensionless).

strain diagram for concrete, as assumed in Clause 47, par. 1, of G.B.V. 1962 – see Fig. 8 (the concrete is unable to resist tensile stresses). The deflection z' will then again be analogous to the compressive strain (shortening) ε_b'. The thickness n corresponds to the maximum compressive strain of the concrete $\varepsilon_u' = 3.5^0/_{00}$.

Other shapes of stress-strain diagrams can be simulated similarly.

With a model as described above it is possible, if the base of the model is geometrically similar to the section to be investigated, to determine the behaviour of a steel or concrete section under the influence of an axial (*i.e.*, centrally applied) load.

If the model represented in Fig. 2 is subjected to a vertical downward force N' whose point of application is located eccentrically, the model will adopt a tilted position, in such a manner that the resultant of the upward pressure is in equilibrium with N'. An upward force N can similarly be applied. In Fig. 9 the model is shown in a tilted position of equilibrium, which was obtained from an initial condition in which the model was immersed in the liquid to half its thickness m. With the aid of this model it is possible to investigate the be-

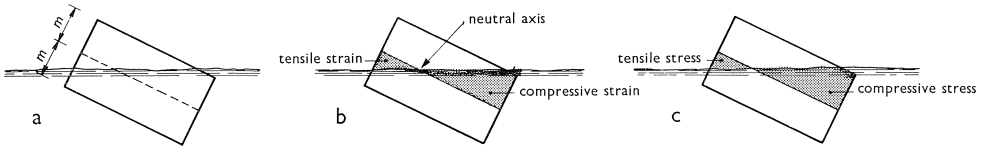

Fig. 9.

haviour of a steel section, geometrically similar to the base of the model, under the influence of an eccentric loading. The following data as to this behaviour can be obtained from the model:

a. the strains at each point of the section (=the amounts of downward or upward deflection) and the position of the neutral axis (see Fig. 9b);
b. the curvature, represented by the rotation angle of the model (see Section 3).

In the case of steel the shape of the compressive stress diagram can also be obtained (see Fig. 9c).

The same applies to a concrete section, provided that it has at least one axis of symmetry. The point of application of N' should be located on this axis, which also indicates the direction of bending. Perpendicular to this direction the model has the triangular cross-sectional shape mentioned above.

2 Model for axially and eccentrically compressed reinforced concrete sections

For determining the strains and stresses in axially and eccentrically compressed reinforced concrete sections having at least one axis of symmetry it is a simple matter to construct a model with the aid of the information given in Section 1.

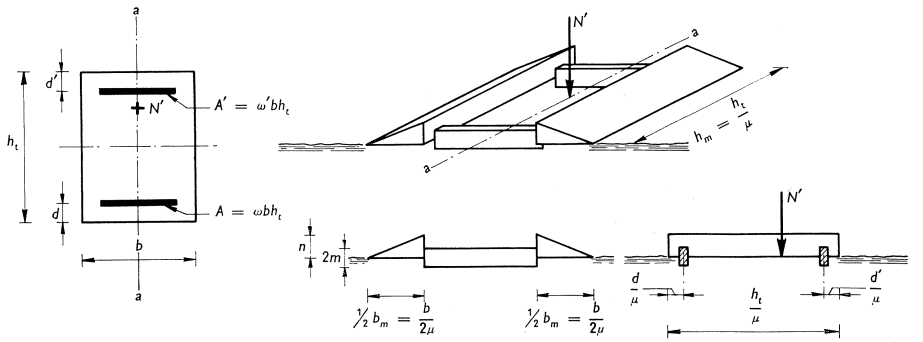

Fig. 10. Model for a rectangular reinforced concrete section.

Fig. 10 [1]) gives an example of a rectangular section (μ = scale factor). When loaded in the manner indicated, the concrete portion of the section will, in the model, have to possess – perpendicular to the axis *a–a* – a triangular vertical cross-sectional shape. For reasons of model testing technique this triangular portion corresponding to the concrete has, in the model, been split up into two prisms. The total base of the prisms is geometrically similar to the section under investigation. As already stated, the thickness n corresponds to the maximum concrete compressive strain $\varepsilon_u' = 3.5^0/_{00}$. The two small connecting beams in the model represent the reinforcement A and A' respectively. The location of these beams in the model corresponds to that of the reinforcement in the actual section. The thickness $2m$ corresponds to the sum $\varepsilon_e + |\varepsilon_e'|$ (*e.g.*, $2 \times 1.143^0/_{00}$ for mild steel with a yield stress of 24 kg/mm², specified QR 24). As the modulus of elasticity of steel is a multiple of that of concrete, the volume of those parts of the model which represent the steel will have to be appropriately enlarged in relation to the concrete part. If the reinforced concrete section is so loaded that everywhere a compressive strain (shortening) $\varepsilon = \varepsilon_u' = 3.5^0/_{00}$ occurs, then:

$$N' = \sigma_u' b h_t + A\sigma_e' + A'\sigma_e'$$

or with $\omega = \dfrac{A}{bh_t}$ and $\omega' = \dfrac{A'}{bh_t}$:

$$\frac{N'}{\sigma_u' b h_t} = 1 + \omega \frac{\sigma_e'}{\sigma_u'} + \omega' \frac{\sigma_e'}{\sigma_u'} \quad \ldots\ldots\ldots\ldots\ldots\ldots \quad (1)$$

If the dimensions of the concrete part have been chosen (*i.e.*, $h_m = h_t/\mu$; $b_m = b/\mu$ and n), then the volume thereof is known. This volume is represented by the term 1 in equation (1). If the concrete and steel qualities (σ_u' and $\sigma_e' = |\sigma_e|$) are given, the ratio of the volume of the steel part to that of the concrete

[1]) Where necessary, the notation of G.B.V. 1962 has been retained, except that $\omega = A/bh_t$ and not $\omega = 100\ A/bh_t\%$ as in G.B.V. 1962.

part can be determined from the right-hand member. Thus the volume of the small connecting beams is known. The thickness $2m$ follows from the thickness n, so that then only the width and length remain to be determined. In order to obtain as accurate a representation of reality as possible, the width of the connecting beams will have to correspond approximately to the diameter of the reinforcement, having due regard to the scale factor. Therefore that width should be adjusted as nearly as possible; the length can then be calculated.

More complex cases, such as T-shaped, circular and diamond-shaped sections (see Fig. 11), can also be investigated, as well as sections in which the steel does not possess a very definite yield point (see Fig. 12). The model of a prestressed concrete section can be constructed as shown in Fig. 13. The shape of the stress-strain diagram of the prestressing steel can suitably be approximated in the manner indicated in Fig. 12. In the unloaded condition the underside of the "concrete part" of the model again coincides with the surface level of the liquid. Prestressing is effected by shifting the part representing the prestressing steel vertically upwards in relation to the liquid surface by such an amount as corresponds to the tensile strain of the prestressing steel.

It is possible in principle to extend the analogy model to include non-symmetrical sections and the case of biaxial bending, but these possibilities will not be examined in the present article.

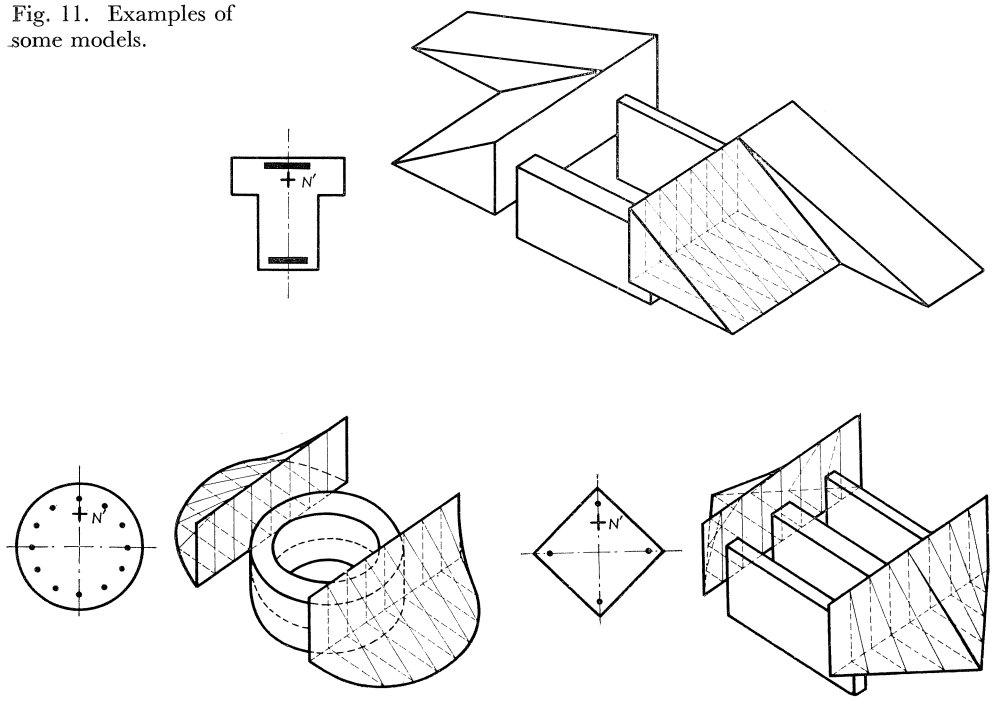

Fig. 11. Examples of some models.

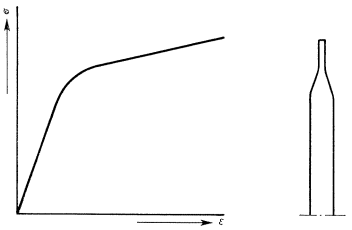

Fig. 12. Model of a type of steel without a definite yield point.

Fig. 13. Model of a prestressed concrete section.
a. unloaded and not yet prestressed;
b. loaded and prestressed.

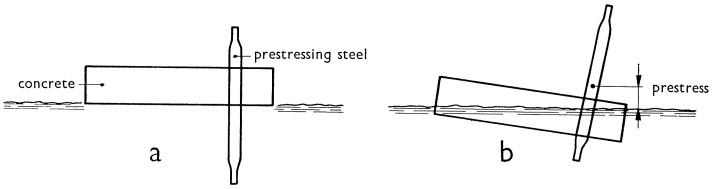

3 Model for axially and eccentrically compressed reinforced concrete members

If the external load N' is applied within the plane through the underside of the concrete part, the model described above will represent the behaviour of a *section*, *i.e.*, the length of a structural member will have no effect on this behaviour. However, if N' is applied higher up, the position of the resultant of the upward pressure will, in the horizontal direction, be affected by the rotation angle φ_m of the model (see Fig. 14).

For the actual section this therefore corresponds to a displacement of the position of the resultant in consequence of the curvature of the axis of the member. This phenomenon plays a part in connection with buckling and can be analysed as follows.

A structural member hinged at the ends and subjected to bending and direct force (longitudinal force) will, under the influence of this loading, deflect in the manner indicated in Fig. 15. According as this loading increases, the eccentricity of the direct force in relation to the axis of the member will increase (buckling). By appropriately choosing the height H in the model (see Fig. 14) it is possible to obtain agreement between the displacement of the resultant in the model and the increasing eccentricity in reality.

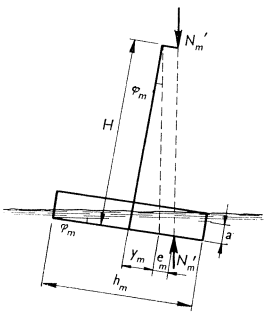

Fig. 14. Introduction of the effect of the length of a structural member by means of the height H in the model.

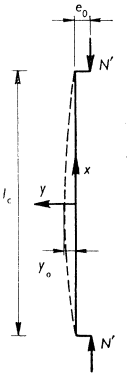

Fig. 15. Eccentrically compressed member.

Assuming a sinusoidal shape for the deflection of the member – see the following article – we may provisionally (see also 5b) write (see Fig. 15):

$$y = y_0 \cos \frac{\pi x}{l_c} \quad \ldots \ldots \ldots \ldots \ldots \ldots \ldots \ldots \ldots \quad (2)$$

For the critical section $x = 0$ we have:

$$\frac{d^2y}{dx^2} = -y_0 \frac{\pi^2}{l_c^2} \quad \ldots \ldots \ldots \ldots \ldots \ldots \ldots \ldots \quad (3)$$

Also:

$$\frac{d^2y}{dx^2} = \frac{\varepsilon_1 - \varepsilon_2}{h_t} \quad \ldots \ldots \ldots \ldots \ldots \ldots \ldots \ldots \quad (4)$$

where ε_1 and ε_2 denote the strains in the extreme fibres and h_t denotes the depth of the section $x = 0$ (the section under consideration) in the direction of bending. From equations (3) and (4) follows:

$$y_0 = \frac{\varepsilon_1 - \varepsilon_2}{h_t} \cdot \frac{l_c^2}{\pi^2} \quad \ldots \ldots \ldots \ldots \ldots \ldots \ldots \ldots \quad (5)$$

Now the eccentricity of the load in the model should correspond to that for $x = 0$ in reality; hence:

$$e_0 + y_0 = \mu(e_m + y_m)$$

or (see Fig. 14):

$$e_0 = \mu e_m$$

and $$y_0 = \mu y_m = \mu H \tan \varphi_m \quad \ldots \ldots \ldots \ldots \ldots \ldots \ldots \quad (6)$$

Substitution of (5) into (6) gives:

$$\frac{\varepsilon_1 - \varepsilon_2}{h_t} \cdot \frac{l_c^2}{\pi^2} = \mu H \tan \varphi_m \quad \ldots \ldots \ldots \ldots \ldots \ldots \quad (7)$$

From Fig. 14 it follows that $a = h_m \tan \varphi_m$. Furthermore $\varepsilon_1 - \varepsilon_2 = a \frac{\varepsilon_u'}{n}$ so that:

$$\frac{d^2y}{dx^2} = \frac{\varepsilon_1 - \varepsilon_2}{h_t} = \frac{\varepsilon_1 - \varepsilon_2}{\mu h_m} = \frac{\varepsilon_u'}{n} \cdot \frac{1}{\mu} \tan \varphi_m$$

This indicates – as already stated – that a rotation in the model corresponds to a curvature in the actual member. Substituted into equation (7) this gives:

$$\frac{1}{\mu} \frac{\varepsilon_u'}{n} \cdot \frac{l_c^2}{\pi^2} \tan \varphi_m = \mu H \tan \varphi_m$$

or

$$H = \frac{l_c^2}{\pi^2} \cdot \frac{1}{\mu^2} \cdot \frac{\varepsilon_u'}{n} \quad \ldots \ldots \ldots \ldots \ldots \ldots \ldots \ldots \quad (8)$$

This value of H can be taken as the starting point for constructing a model. Because of the not entirely correct assumption contained in equation (2), however, the test results obtained must subsequently be corrected, as is to be discussed in 5b.

It is therefore possible, in the manner indicated above, to ascertain the behaviour of a reinforced concrete column under the action of an external axial or eccentric load. Not only can the maximum attainable value of N' (= the ultimate load N_{br}') be determined, but also the associated position of the neutral axis, the strains ε_1 and ε_2 at the extreme fibres (see Figs. 5b and 5c), and the deflection can be represented in a manner that can be visualized. And this can, of course, be done for any other value of N'. With one and the same model it is possible to investigate the behaviour of a series of columns having the same cross-section but different values of the initial eccentricity of the load and different lengths. The behaviour of steel columns and prestressed concrete columns can also be investigated in similar fashion.

In principle, other boundary conditions, such as resilient (semi-rigid) restraint, may be included in the investigation.

4 Model technique

The liquid used in conjunction with the models tested was water. The models were made of a light and easily workable material, namely, foamed polystyrene. Although this material in itself absorbs little water, it was found to be necessary to reduce this water absorption. Treatment of the exterior of the material with wax had the desired effect – at any rate, so long as the wax had not dried up. Is was also found that this treatment so reduced the surface tension between the model material and the water that the effect thereof on the behaviour of the model was entirely negligible.

In all the models the scale factor was $\mu = 1$. Initially a thickness $n = 3.5$ cm was adopted for the "concrete part", but this entailed a not quite acceptable dimensional inaccuracy and deficient stiffness of this part where it tapers off to zero thickness. For this reason a scale was adopted in which 2 cm corresponded to $1^0/_{00}$ strain, so that $n = 7$ cm. No difficulties were encountered with this scale.

The weight of a model was so low that it was quite a simple matter to adjust the requisite centre of gravity and the weight to the correct position and correct value respectively by applying a small weight which was always under water.

A "bridge", likewise made of foamed polystyrene, was placed upon the model. By means of this device the point of application of the external load could be adjusted to the desired height and position. According to equation (8) the height H associated with $\mu = 1$ is:

$$H = \frac{l_c^2}{\pi^2} \cdot \frac{3{,}5 \cdot 10^{-3}}{7} \approx \frac{l_c^2}{20.000}.$$

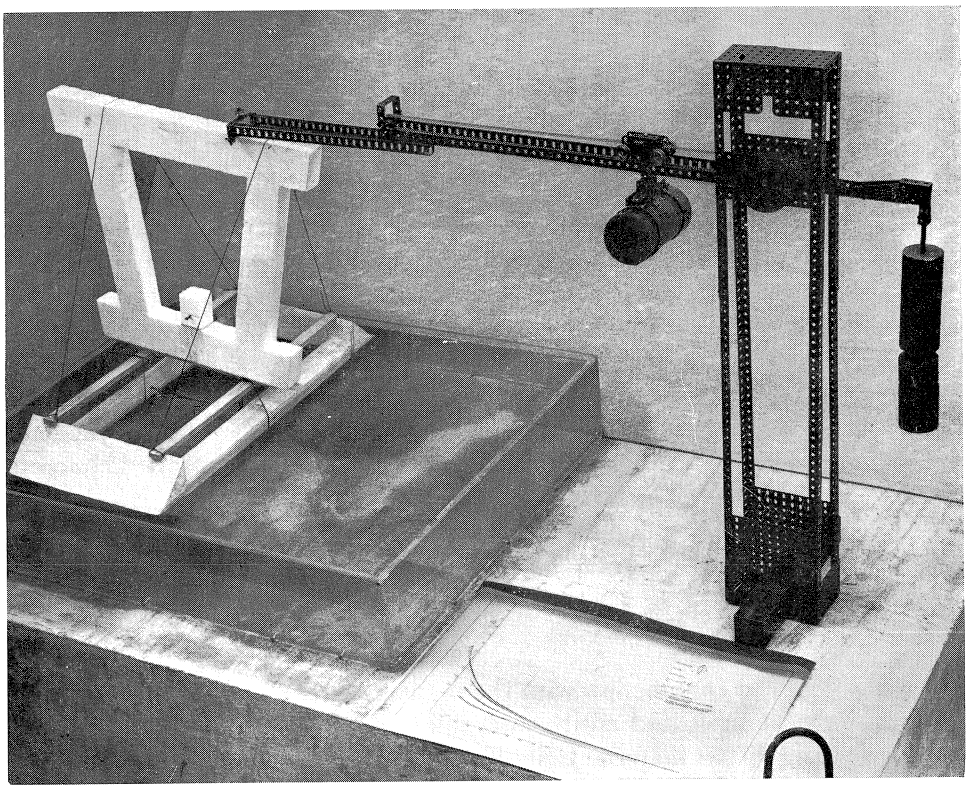

Fig. 16a and b. General view of the test arrangement.

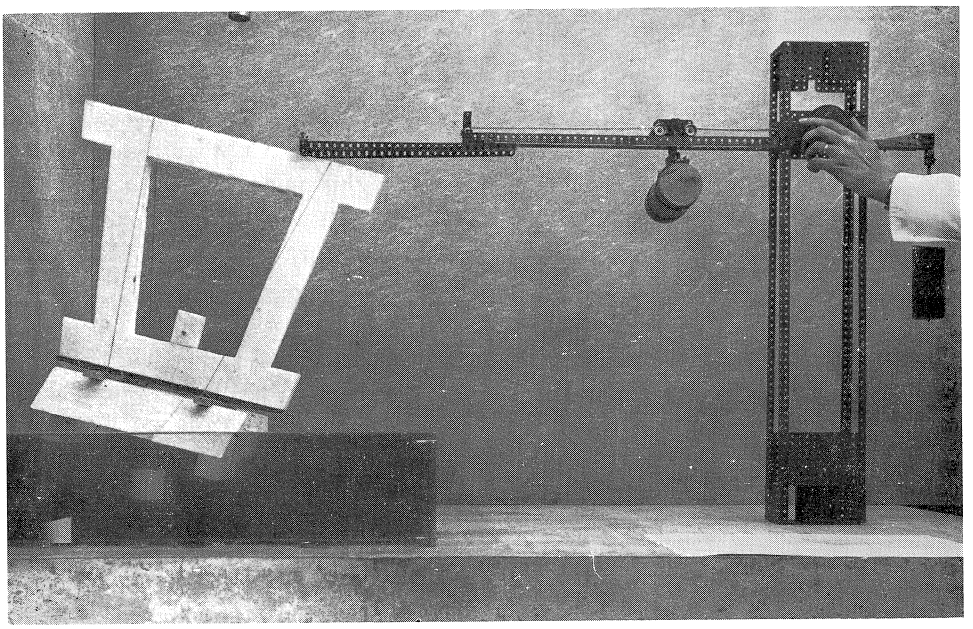

Hence for a length $l_c = 3.00$ m we have $H \approx 4.5$ cm, and for $l_c = 10.00$ m we have $H \approx 50$ cm. These dimensions can suitably be produced in a model. The bridge was so balanced at its centre of gravity that it was possible to exert a vertical upward force also when the model was displaced horizontally.

The load was applied by means of a lever along which a weight could be shifted without having to touch the lever by hand, so that accurate adjustment was possible. Figs. 16a and 16b give a general view of the test arrangement.

The desired quantities to be determined, such as the strains at the extreme fibres and the position of the neutral axis, were measured by means of small measuring rods. The imposed load was read directly from a scale extending along the lever.

5 Model errors

a. Correction of the load N_m' (see Fig. 17).

If the model had an infinitely small thickness (n), then $\varphi_m \to 0$, $\cos \varphi_m \to 1$ and $\sin \varphi_m \to 0$. In that case:

$$\Sigma M = 0 \to N_m' e_m + N_m' y_m = N_m' \cdot p_m \quad . \quad (9)$$

The point 0 in the model corresponds to the centroid of the actual section. For this section equation (9) signifies that a direct force N' occurs at a distance $p = \mu p_m$ from the centroid. The model would correctly represent the prototype.

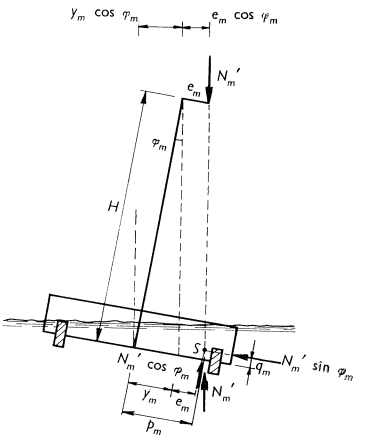

Fig. 17. Correction of N_m'.

Since the model has a finite thickness n, however, the rotation φ_m may acquire values that are not negligible. Also, since the point of application s of the resultant of the upward pressure is not located in the plane through the underside of the concrete part, an additional moment $N_m' q_m \sin \varphi_m$ is found to occur. Hence in this case:

$$\Sigma M = 0 \to N_m' e_m \cos \varphi_m + N_m' y_m \cos \varphi_m =$$

$$= N_m' \cos \varphi_m p_m + N_m' q_m \sin \varphi_m \quad . \quad . \quad . \quad . \quad . \quad . \quad . \quad . \quad . \quad . \quad . \quad (10)$$

For the actual section this signifies (apart from the small error $N_m' q_m \sin \varphi_m$) that it is loaded at a distance $p = \mu p_m$ from the centroid by a direct force of the magnitude $N_m' \cos \varphi_m$ in the model – *i.e.*, the force N_m' read on the scale affixed to the lever must be corrected with the relevant value of $\cos \varphi_m$. With regard to the term $N_m' q_m \sin \varphi_m$ it can be stated that both q_m and $\sin \varphi_m$ are small.

b. Correction of the height H and the initial eccentricity e_m (or e_0 as the case may be).

As stated on page 9, the assumption embodied in equation (2) is not quite correct. For $x = {}^1/_2\, l_c$ we have $y = e_0$ and therefore $M = N' e_0$ (see Fig. 15). From equation (2), however, it also follows for the same section:

$$\frac{d^2y}{dx^2} = y_0 \frac{\pi^2}{l_c^2} \cos\frac{\pi}{2} = 0,$$

so that M would have to be zero. A better approximation, as is also being adopted in the following article, page 20, can be obtained with (see Fig. 18):

$$y = y_0 \cos\frac{\pi x}{L} = y_0 \cos\frac{\pi x \vartheta}{l_c} \quad \ldots\ldots\ldots\ldots\ldots\ldots \quad (11)$$

where $\dfrac{l_c}{L} = \vartheta \leqq 1$ and $y_0 = e_0 + f$.

The following expressions conform to those derived on pp. 20–21:

$$\frac{y_0}{h_t} = \frac{(\varepsilon_1 - \varepsilon_2)}{\pi^2 \vartheta^2} \left(\frac{l_c}{h_t}\right)^2 = \left(\frac{1}{\Xi} + \frac{1}{\Phi}\right)(\varepsilon_1 - \varepsilon_2) \left(\frac{l_c}{h_t}\right)^2 \quad \ldots\ldots\ldots \quad (12)$$

$$\frac{e_0}{h_t} = \frac{(\varepsilon_1 - \varepsilon_2)}{\Xi} \left(\frac{l_c}{h_t}\right)^2 \quad \ldots\ldots\ldots\ldots\ldots\ldots\ldots\ldots \quad (13)$$

$$\frac{f}{h_t} = \frac{(\varepsilon_1 - \varepsilon_2)}{\Phi} \left(\frac{l_c}{h_t}\right) \quad \ldots\ldots\ldots\ldots\ldots\ldots\ldots\ldots \quad (14)$$

where ε_1 and ε_2 again represent the strains at the extreme fibres for $x = 0$, and Ξ and Φ are functions of ϑ only – see Table I (page 21). Furthermore:

$$\frac{y_0}{h_t} = \frac{y_m}{h_m} \quad \ldots\ldots\ldots\ldots\ldots\ldots\ldots\ldots \quad (12a)$$

$$\frac{e_0}{h_t} = \frac{e_m}{h_m} \quad \ldots\ldots\ldots\ldots\ldots\ldots\ldots\ldots \quad (13a)$$

$$\frac{f}{h_t} = \frac{f_m}{h_m} \quad \ldots\ldots\ldots\ldots\ldots\ldots\ldots\ldots \quad (14a)$$

From equations (12) and (12a) we obtain:

$$\frac{y_m}{h_m} = \left(\frac{1}{\Xi} + \frac{1}{\Phi}\right)(\varepsilon_1 - \varepsilon_2) \left(\frac{l_c}{h_t}\right)^2$$

In this equation l_c, h_t and h_m are known. For a certain load applied to the model, y_m, ε_1 and ε_2 can be measured. The value of $\left(\dfrac{1}{\Xi} + \dfrac{1}{\Phi}\right)$ can be calculated, and then ϑ can be determined by means of the above-mentioned table. The values of $1/\Xi$ and $1/\Phi$ separately are then also known. The associated initial eccentricity

e_0' or e_m' can be determined by means of equations (13) and (13a). The value e_m' will not be equal to the value e_m adjusted in the model. As a result of introducing equation (11) the value of H, instead of conforming to equation (8), becomes:

$$H' = \frac{l_c^2}{\pi^2 \vartheta^2} \cdot \frac{\varepsilon_u'}{n} \cdot \frac{1}{\mu^2} \quad \ldots \ldots \ldots \ldots \ldots \ldots \ldots \quad (8a)$$

As the value of ϑ was already known, it would also be possible to correct the value of H.

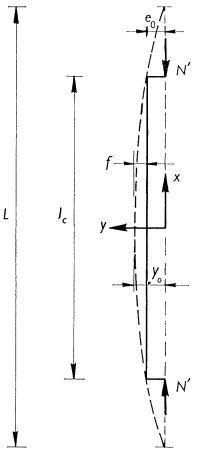

Fig. 18. Eccentrically compressed member.

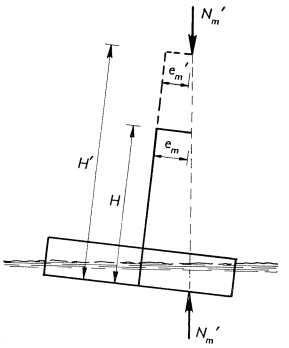

Fig. 19. Correction of H and e_m.

To summarise, it can be said that at the start of the test the height H according to equation (8) is available, the initial eccentricity being adjusted to a value e_m (or e_0). These quantities must subsequently be corrected with the test results obtained. From Fig. 19 it is apparent that this degree of freedom is indeed available. No change occurs in the state of equilibrium if H and e_m are replaced by H' and e_m'.